Selected papers presented at the 14th Symposium of Magnetic Measurements and Modelling SMMM'2023

Designing an Improved Method to Determine the Anhysteretic Curve in Soft Magnetic Materials via the Jiles–Atherton Model

Z. Roubal* and V. Smejkal

Department of Theoretical and Experimental Electrical Engineering, Brno University of Technology, Technická 12, 612 00 Brno, Czech Republic

Doi: 10.12693/APhysPolA.146.51 *e-mail: roubalz@vutbr.cz

The article discusses a novel procedure for measuring the anhysteretic curve in soft magnetic materials. This curve frequently finds use in diverse applications, such as the Jiles–Atherton hysteresis model. The actual method is characterized in detail, including sample calculations for materials exhibiting various hysteresis loop shapes (ferrites, grain-oriented steel, and nanocrystalline material). To illustrate the benefits of the proposed approach, the authors compare the measurement-based and the simulated curves, the latter being obtained through an optimal interleaving of the model.

topics: anhysteretic curve, Jiles–Atherton hysteresis model, magnetic measurement.

1. Introduction

Hysteresis loop modeling embodies an important task in the analysis of various electrical circuits containing ferromagnetic cores. The applications include, for example, the transient behavior of classic power transformers and the research of switching power supplies. Several descriptions of hysteresis loops are available, including the Preisach mathematical model [1, 2] or the Jiles–Atherton (J-A) formalism [3], often implemented in SPICE-like simulation software. The parameter determination procedure of the Jiles–Atherton model presented in [3] may diverge in some cases. Thus, in a previously published experimental project [4], some modifications of the classic Jiles–Atherton model were analyzed using the least squares method in order to yield an improved hysteresis loop of the nanocrystalline material VITROPERM 500F. Here, the anhysteretic magnetization curve was obtained as an average of the upper and lower parts of the limiting hysteresis loop and was therefore not measured. The differences between the measured loop and that simulated via the Jiles–Atherton model were compared. The problem with the Jiles–Atherton model in approximating the VITROPERM 500F material rests in the rapid transition to saturation, dissimilar from the gradual transition of the Langevin equation [4]. Other sources use different initial approximations of the Jiles–Atherton model's parameters [5–9]. An overview of the state of the art is proposed in [10].

2. Tools for the magnetic curve measurements

The setup shown in Fig. 1 allowed us to characterize the primary magnetization curve, the quasi-static and dynamic hysteresis loop group, and the anhysteretic curve. The original set of instruments [11] was modified by using a more effective analog-to-digital (A/D) sampling device and a voltage-to-current (V/I) converter to deliver high-quality demagnetization of the sample and to measure the anhysteretic curve reliably; in small thorium samples, an automatically zeroed buffer amplifier is applicable [12]. A Siglent SDG2042X DDS generator with the true form technology was utilized to generate the required waveform, providing a sufficient resolution (14-bit) to expose the demagnetization waveform. The generator then excited a V/I converter, developed previously at the Department of Theoretical and Experimental Electrical Engineering (DTEEE) to facilitate magnetic measurements. In the converter, an OPA541 operational amplifier (OA) with a precision-sensing resistor in a Howland circuit is integrated. The requirements comprised a grounded output, stability of the zero converter (a prerequisite for compensation), and high output resistance. The stability at inductive loads was ensured. Generally, the sample can be a toroid or an Epstein frame. The current excites the magnetizing winding N_1 and is sensed at the shunt R_B. An electronic fluxmeter is connected

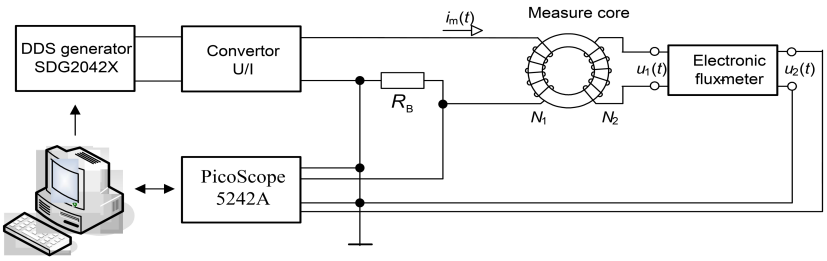

Fig. 1. The measuring setup.

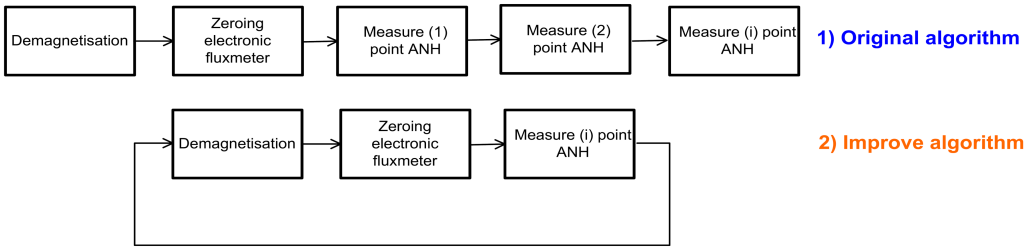

Fig. 2. The conventional and the improved algorithms.

to the secondary measuring winding N_2. The signals are converted into digital form using a 12-bit PicoScope 5242A oscilloscope. In quasi-hysteresis loop measurements, a 30 Hz low-pass filter is set to suppress the 50 Hz mains interference and other spurious effects from, for example, the switching power supply. The data are transferred via a USB[†1] interface to a PC[†2], where the processing is performed in MATLAB.

The measuring configuration is applicable up to a frequency of 5 kHz. At higher frequencies, a voltage amplifier appears to be more advantageous than a V/I converter, providing a harmonic excitation waveform of the magnetic flux density B. Then, measurements up to 100 kHz are feasible with a passive integrator.

3. Improving the algorithm to measure the anhysteretic curve

The various algorithms to measure the anhysteretic curve described in [13] are very demanding in terms of the stability of the zero of the electronic fluxmeter. Multiple measurement variants are possible, assuming three or two windings. When a quasi-static hysteresis loop requiring a processing time of 40 s is measured, we can execute a program-based correction of the measured data if the curve is closed [11]. The stored zero correction is also usable in measuring the initial magnetization curve. This option cannot be employed in an anhysteretic curve or, for example, where the total measurement time corresponds to 30 min and/or the samples are very small (an electronic fluxmeter range of less than 3 mWb) — such a procedure would render the results generally inapplicable.

Thus, in contrast to the original version of the point-by-point sequential measurement, demagnetizing the measured sample and zeroing the electronic fluxmeter took place between each measurement point (Fig. 2). As a result, the requirements for the stability of the electronic fluxmeter zero resemble those that relate to measuring the initial magnetization curve. The signal waveform to enable a single point measurement of the anhysteresis curve is described within

$$i_1(t) = I_{\max}\, \mathrm{e}^{-tA} \sin(2\pi f t) + I_{\mathrm{DC}} \left(1 - \mathrm{e}^{-\frac{t}{\tau}}\right), \tag{1}$$

where $I_{\max}$ is the maximum amplitude of the demagnetization signal, A denotes the amplitude decay constant, f refers to the frequency, I_{DC} represents the setpoint of the anhysteretic curve, and τ is the time constant of the setpoint. Regarding the experimentally preset values to ensure an optimum demagnetization of the sample, the waveform is shown in Fig. 3.

In the selected samples (including the oriented steel Sonaperm, Trafoker S, NiZn ferrite Amidon 43, and nanocrystalline material VITROPERM 500F), the measuring signal parameters read $I_{\max} = 0.6$ A, $A = 0.06$, $f = 1$ Hz, $\tau = 1$ s.

[†1] USB — Universal Serial Bus
[†2] PC — personal computer

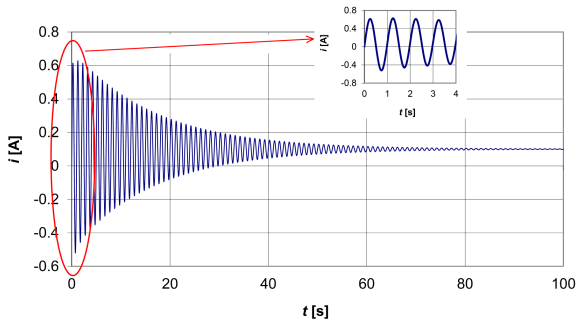

Fig. 3. The measured magnetization signal.

Further, I_{DC} equals zero at demagnetization but then gradually increases until the material is saturated.

In addition to the fluxmeter zero stability issues, we encountered problems with the V/I converter offset in materials having a nearly orthogonal hysteresis loop (Trafoker S). The favorable design, however, allowed the offset converter V/I to exhibit an offset below 20 μA.

The setup also includes a thermocouple to measure the temperature of the sample, similar to the scenario described in [14].

4. The Jiles–Atherton (J-A) hysteresis loop model

The initial equation to characterize this model is one that exposes the behavior in the magnetic material at the domain level. More concretely, the equation embodies a differential description that changes the output according to the varying direction of the input variable, namely the magnetic field strength. The total magnetization M is then given by

$$M = M_{irr} + M_{rev}, \tag{2}$$

where M_{irr} is the irreversible and M_{rev} the reversible magnetization. When the magnetization changes, irreversible shifts occur; these are defined by

$$\frac{\mathrm{d}M_{irr}}{\mathrm{d}H} = \frac{M_{an} - M_{irr}}{k\delta - \alpha\,(M_{an} - M_{irr})}. \tag{3}$$

In (3), M_{an} and M_{irr} denote the lossless (anhysteretic) and the irreversible magnetization, respectively; k is the parameter determining the curve broadening (i.e., the hysteresis losses); δ represents the sign parameter; and α represents the molecular field parameter [3]. The sign function δ follows the change in the direction of the magnetic field strength and is thus specified via

$$\delta = \begin{cases} +1, & \text{for} \quad \frac{\mathrm{d}H}{\mathrm{d}t} > 0, \\ -1, & \text{for} \quad \frac{\mathrm{d}H}{\mathrm{d}t} < 0. \end{cases} \tag{4}$$

Lossless magnetization is an ideal process where no disturbances in the crystal lattice (causing the losses) occur during the magnetization; its actual progress is thus determined by the displacement of the domain walls and the rotation of the spontaneous magnetization of the domains in the direction of the external field. This dependence is most often given by the Langevin function

$$M_{an} = M_{sat}\left[\coth\left(\frac{H_{ef}}{a}\right) - \frac{a}{H_{ef}}\right] = M_{sat}\left[\coth\left(\frac{H+\alpha M}{a}\right) - \frac{a}{H+\alpha M}\right], \tag{5}$$

where M_s is the saturation magnetization (a characteristic of each material, temperature-dependent), a [A/m] denotes the temperature-dependent shape parameter, and H_{ef} stands for the total magnetic field strength; this strength is obtained from the sum of the external field H and the internal (Weiss) field, which is $-\alpha$ times the magnetization M. The parameter α takes on values of the order of approximately 10^{-3} to 10^{-7}. As proposed in [5], (5) was derived for paramagnetic materials and thus does not always approximate the waveform exactly. Then, in some cases, other dependencies are used, such as the Brillouin function given by

$$M_{an} = M_{sat}\cdot\left[\frac{2J+1}{2J}\cosh\left(\frac{2J+1}{2J}\,\frac{H_{ef}}{a}\right) - \frac{1}{2J}\cosh\left(\frac{1}{2J}\,\frac{H_{ef}}{a}\right)\right], \tag{6}$$

where J [-] is the quantum number, a quantity that takes discrete values from 0.5 to ∞ [15], and α [A/m] has a meaning different from that in (5). In general, such a function can be any monotonic increasing function passing through zero and limiting to $\mp M_s$ for H_{ef} going to $\mp\infty$. If the waveform is measured, the obtained values can be applied.

The last part of (2) is reversible magnetization, expressed in the model as the difference between the lossless and the irreversible magnetization, which is attenuated [2], i.e.,

$$M_{rev} = c\,(M_{an} - M_{irr}), \tag{7}$$

where the parameter c belongs to the interval $0 < c < 1$. The resulting formula, which shows the magnetization change with the magnetic field strength variation, is formed by a derivative of (1), an addition to (2), and a derivative of (3); therefore,

$$\frac{\mathrm{d}M}{\mathrm{d}H} = \frac{\mathrm{d}M_{irr}}{\mathrm{d}H} + \frac{\mathrm{d}M_{rev}}{\mathrm{d}H} = \frac{\mathrm{d}M_{irr}}{\mathrm{d}H} + c\left(\frac{\mathrm{d}M_{an}}{\mathrm{d}H} - \frac{\mathrm{d}M_{irr}}{\mathrm{d}H}\right) = (1-c)\,\frac{M_{an}-M_{irr}}{k\delta - \alpha\,(M_{an}-M_{irr})} + c\,\frac{\mathrm{d}M_{an}}{\mathrm{d}H}. \tag{8}$$

The magnetization waveform M corresponding to the input waveform of the magnetic field strength H is then computed similarly to the procedure

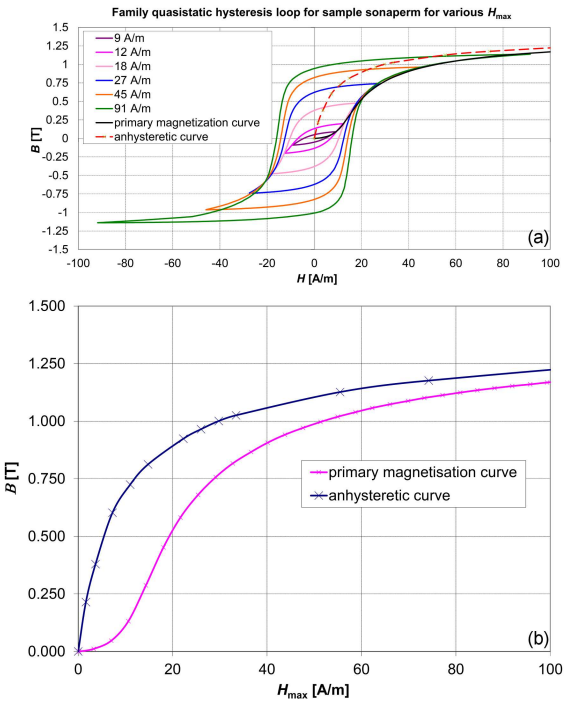

Fig. 4. The measuring hysteresis loop group, initial magnetization curve (a), and anhysteretic curve for the Sonaperm material (b).

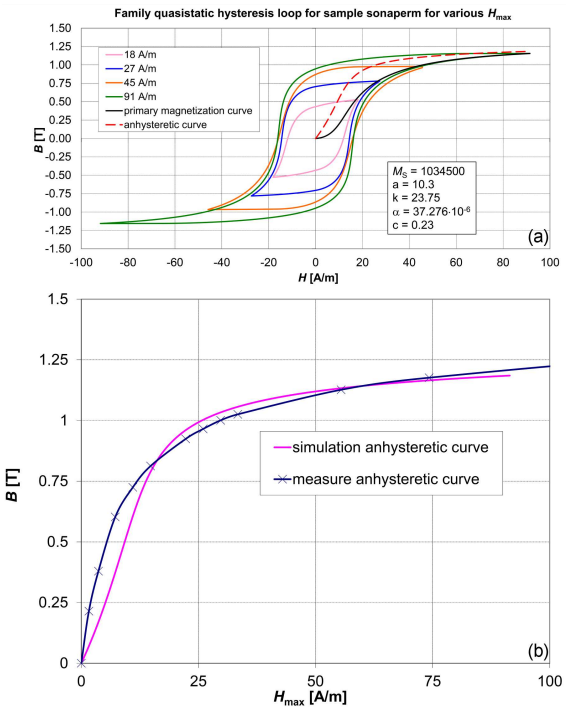

Fig. 5. The simulation hysteresis loop, initial magnetization curve (a), and anhysteretic curve for the Sonaperm material (b).

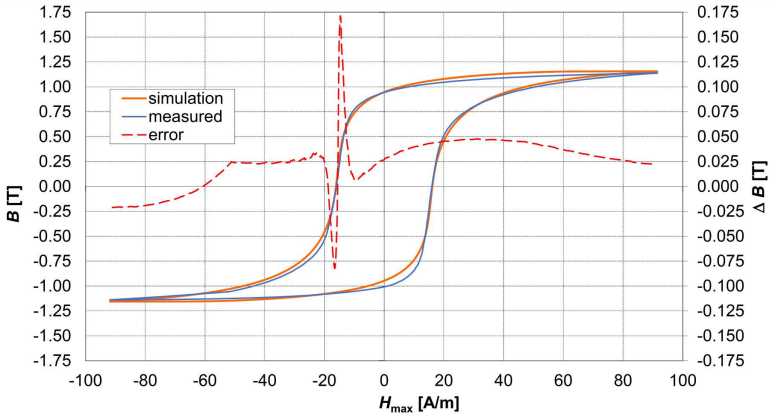

Fig. 6. Comparison of measured and simulated limiting hysteresis loop for the Sonaperm material. The error is calculated for the upper part of the hysteresis loop.

described in [4]: First, the lossless magnetization value is determined, according to options such as that from (5). Next, the change of the irreversible magnetization is established (3). Now, the reversible magnetization (7) is calculated, allowing us to express the resulting magnetization change according to (8). However, the previous values have already been entered, which means that the calculation can be carried out directly. The disadvantage is that an iterative method needs to be employed in the calculation, because the calculated value determined from the derivative of the magnetization and its preceding values appears in the result. During the procedure, we have to check whether the reversible magnetization (2) is smaller than the lossless magnetization in the first quadrant and, similarly, in the third quadrant when the magnetization field strength decreases from the top of the curve.

If the condition is not applied, the magnetization increases where the magnetic field intensity is reduced from the top of the loop, a process that does not correspond to the actual behavior of the magnetic material. In view of the above details, it can be concluded that obtaining the model parameters is not a simple task. It is possible to use the

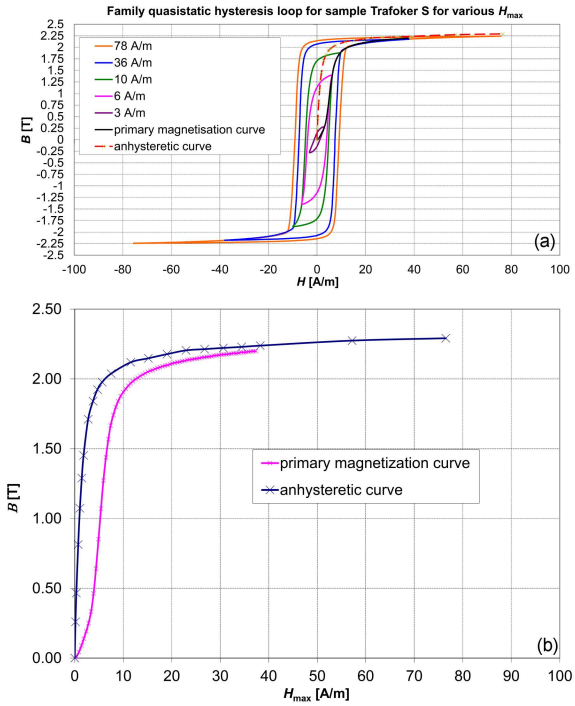

Fig. 7. The measuring hysteresis loop group, initial magnetization curve (a), and anhysteretic curve for the Trafoker S material (b).

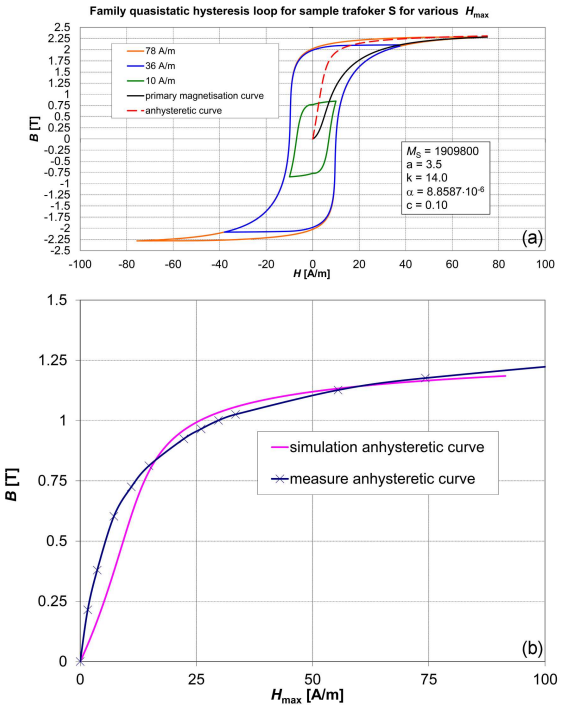

Fig. 8. The simulation hysteresis loop, initial magnetization curve (a), and anhysteretic curve for the Trafoker S material (b).

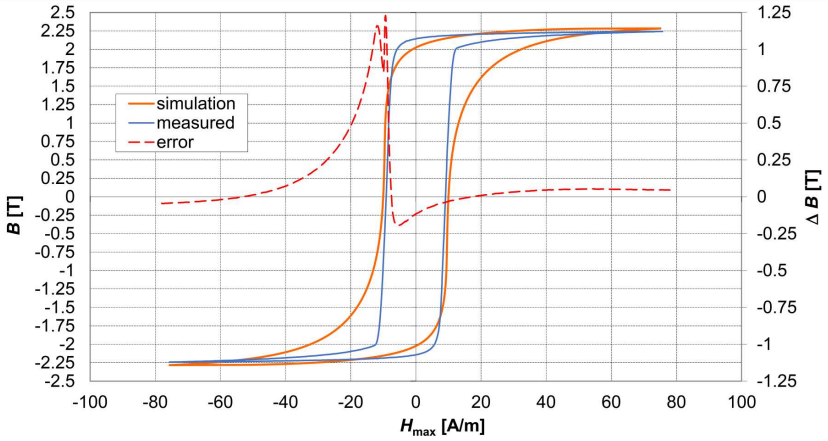

Fig. 9. Comparison of measured and simulated limiting hysteresis loop for the Trafoker S material. The error is calculated for the upper part of the hysteresis loop.

estimation of initial model values from [3] and [6] and then perform their parametric tuning using the least squares method for the best curve fitting.

5. The measured anhysteretic curve as compared with the model

All of the quasi-static hysteresis loops were measured for a period of 40 s, when the influence of eddy currents can be ignored. The excitation signal H was harmonic. A sample of an older oriented Sonaperm tail was used to verify the agreement of the anhysteretic curve measured via a modified algorithm and optimized for the best fit of the hysteresis loop group and the primary magnetization curve (Fig. 4). Such a scenario was employed due to the transition to saturation being more gradual than that of the modern oriented sheets. The toroidal sample had an outer diameter of 110 mm, an inner diameter of 70 mm, and a height of 20 mm. The magnetizing and the measuring winding, N_1 and N_2, had 100 and 50 turns, respectively.

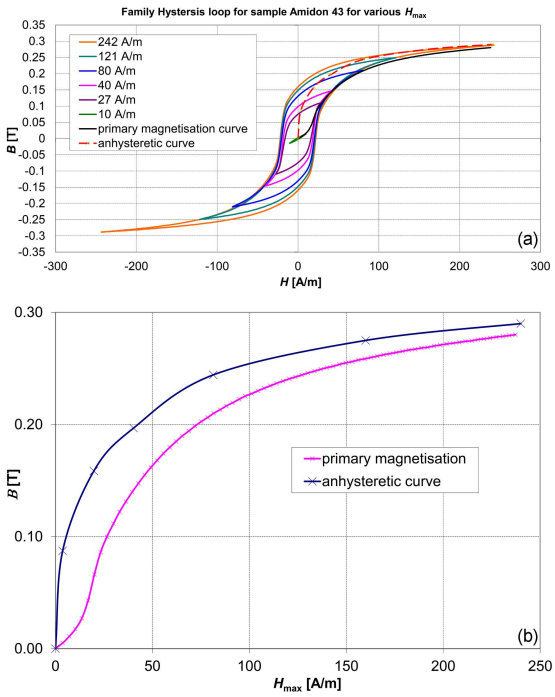

Fig. 10. The hysteresis loop group, initial magnetization curve (a), and anhysteretic curve for the MnZn ferrite material Amidon 43 (b).

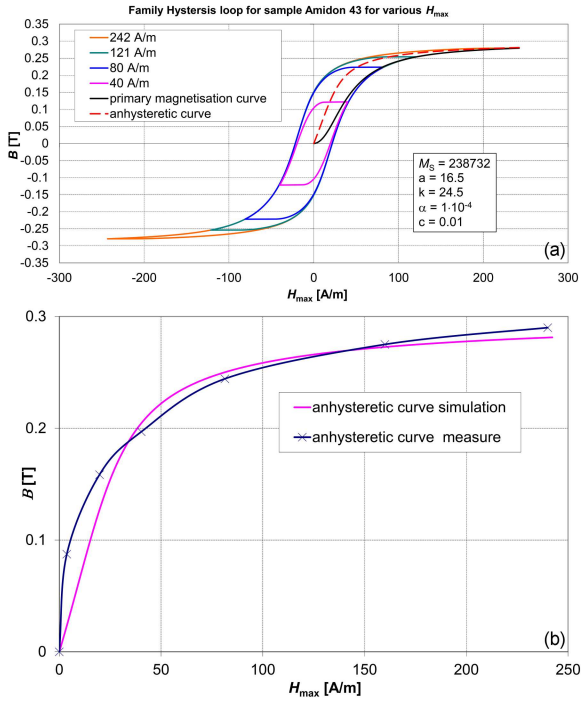

Fig. 11. The simulation hysteresis loop, initial magnetization curve (a), and anhysteretic curve for the ferrite material Amidon 43 (b).

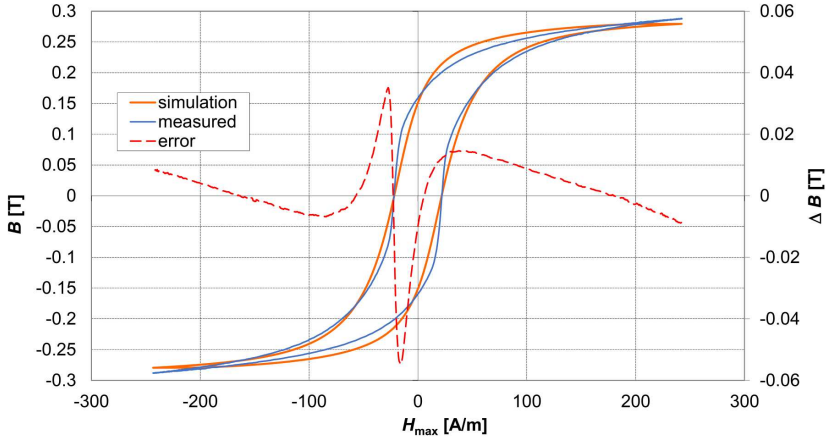

Fig. 12. Comparison of measured and simulated limiting hysteresis loop for the ferrite material Amidon 43.

The optimal parameters of the Jiles–Atherton model were determined in MATLAB by means of the least squares method (Fig. 5). The procedure indicated good agreement with the Langevin function and satisfactory progression of the optimized anhysteretic curve; the largest differences were found in low values of $H_{\max}$ (Fig. 6).

Subsequently, a calculation was performed for the more modern HI-B oriented silicon steel Trafoker S, showing that the J-A model with the Langevin function is practically unable to express the shape of the rectangular hysteresis loop (Figs. 7–9). Using a measured anhysteretic loop did not yield a better approximation. The toroidal sample had an outer diameter of 150 mm, an inner diameter of 110 mm, and a height of 30 mm. The magnetizing winding N_1 and the measuring winding N_2 had 150 and 100 turns, respectively.

The NiZn ferrite Amidon 43 possesses a hysteresis loop with a specific shape (Fig. 10). The initial permeability region is well characterized, but the sharp sides of the hysteresis loop are not visualized at all in the result (Figs. 11 and 12). Again, the measured anhysteretic loop appears to be steeper at the lower values of H.

The Jiles–Atherton model's parameters related to the individual materials. TABLE I

Material	M_s [A/m]	a [A/m]	α ($\times 10^{-6}$)	k [A/m]	c [–]
Sonamperm	1034500	10.3	37.276	23.75	0.23
Trafoker S	1909800	3.5	8.8587	14.0	0.10
Amidon 45	238732	16.5	100	24.5	0.01
Vitroperm 500F	–	–	1	0.75	0.01

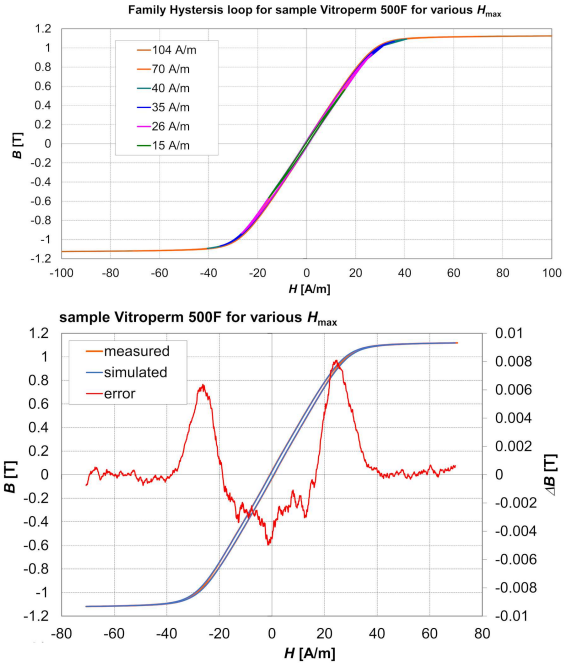

Fig. 13. The measuring hysteresis loop group for Vitroperm 500F (a) and the simulation relating to the measuring anhysteretic curve (b).

The toroidal sample had an outer diameter of 73.7 mm, an inner diameter of 38.9 mm, and a height of 12.7 mm. The magnetizing winding N_1 and the measuring winding N_2 had 135 and 44 turns, respectively.

The Vitroperm 500F nanocrystalline material exhibits a specific shape of the hysteresis loop, is very narrow, and saturates quickly (Fig. 13). Here, the measured anhysteretic loop should be ideally employed in the model to deliver a very small deviation between the measured and the simulated hysteresis loops. The toroidal sample showed an outer diameter of 30 mm, an inner diameter of 20 mm, and a height of 10 mm. The magnetizing winding N_1 had 8 turns, and the measuring winding N_2 had 200 turns.

6. Conclusions

The article presents an algorithm to measure an anhysteretic loop, outlining the typical hysteresis loop shapes (a smooth transition to saturation in the Sonaperm material, sharp transition and right-angled hysteresis loop in Trafoker S, spherical shape in Amidon 43, and a narrow hysteresis loop and sharp transition to saturation in Vitroperm 500F). The characteristics of the materials involved in the project are compared in terms of their characteristics and capabilities (Table I). By extension, the authors discuss the possible limits of the J-A hysteresis loop model. Generally, in strongly anisotropic materials such as Vitroperm 500F, the Langevin function is unsuitable, as it was derived for isotropic materials. Future research is planned to verify our description, modifying the characterization of the anhysteretic curve in accordance with the guidelines proposed in [16]. The procedures exposed herein involved an anhysteretic curve in the form of a table, ensuring the best approximation for the Vitroperm 500F material. The approximation error for the limiting hysteresis loop was below 0.8%.

References

[1] J. Eichler, M. Novák, M. Košek, *Acta Phys. Pol. A* **136**, 713 (2019).

[2] M. Novák, *Acta Phys. Pol. A* **136**, 731 (2019).

[3] D. Jiles, J. Thoelke, M. Devine, *IEEE Trans. Magn.* **28**, 27 (1992).

[4] Z. Roubal, V. Smejkal, in: *2013 9th Int. Conf. on Measurement*, 2013, p. 127.

[5] M. Novák, Ph.D. thesis, Technical University of Liberec, Liberec (Czech Republic) 2003.

[6] D. Lederer, H. Igarashi, A. Kost, T. Honma, *IEEE Trans. Magn.* **35**, 1211 (1999).

[7] K. Hergli, H. Marouani, M. Zidi, *Phys. B Cond. Matter* **549**, 74 (2018).

[8] K. Chwastek, J. Szczyglowski, *Math. Comput. Simulat.* **71**, 206 (2006).

[9] G. Xue, H. Bai, T. Li, Z. Ren, X. Liu, C. Lu, *Mathematics* **10**, 4431 (2022).

[10] R. Szewczyk, *AIP Conf. Proc.* **2131**, 020045 (2019).

[11] Z. Roubal, P. Marcon, M. Čáp, in: *Proc. 9th Int. Conf. 2012 ELEKTRO*, 2012, p. 460.

[12] T. Hejtmánek, Z. Roubal, in: *2021 13th Int. Conf. on Measurement*, 2021, p. 228.

[13] M. Nowicki, *Materials* **11**, 2021 (2018).

[14] T. Charubin, M. Urbański, M. Nowicki, in: *Recent Advances in Systems, Control and Information Technology: Proc. of the Int. Conf. SCIT 2016*, 2016, p. 593.

[15] K. Chwastek, *J. Physics D Appl. Phys.* **43**, 015005 (2009).

[16] R. Szewczyk, *Materials* **7**, 5109 (2014).